

Near-threshold $\Lambda(1520)$ production by the $\vec{\gamma}p \rightarrow K^+\Lambda(1520)$ reaction at forward K^+ angles

H. Kohri¹, D.S. Ahn^{1,2}, J.K. Ahn², H. Akimune³, Y. Asano⁴, W.C. Chang⁵, S. Daté⁶, H. Ejiri^{1,6}, S. Fukui⁷, H. Fujimura^{8,9}, M. Fujiwara^{1,4}, S. Hasegawa¹, K. Hicks¹⁰, A. Hosaka¹, T. Hotta¹, K. Imai⁹, T. Ishikawa¹¹, T. Iwata¹², H. Kawai¹³, Z.Y. Kim⁸, K. Kino^{1,a}, N. Kumagai⁶, S. Makino¹⁴, T. Matsuda¹⁵, T. Matsumura^{16,1,4}, N. Matsuoka¹, T. Mibe^{1,4,10}, M. Miyabe⁹, Y. Miyachi¹⁷, M. Morita¹, N. Muramatsu^{4,1}, T. Nakano¹, S.i. Nam¹⁸, M. Niiyama⁹, M. Nomachi¹⁹, Y. Ohashi⁶, H. Ohkuma⁶, T. Ooba¹³, D.S. Oshuev^{5,b}, C. Rangacharyulu²⁰, A. Sakaguchi¹⁹, T. Sasaki⁹, P.M. Shagin²¹, Y. Shiino¹³, A. Shimizu¹, H. Shimizu¹¹, Y. Sugaya¹⁹, M. Sumihama^{19,4}, A.I. Titov²², Y. Toi¹⁵, H. Toyokawa⁶, A. Wakai²³, C.W. Wang⁵, S.C. Wang⁵, K. Yonehara^{3,c}, T. Yorita^{1,6}, M. Yoshimura²⁴, M. Yosoi^{9,1}, and R.G.T. Zegers²⁵

(LEPS Collaboration)

¹Research Center for Nuclear Physics, Osaka University, Ibaraki, Osaka 567-0047, Japan

²Department of Physics, Pusan National University, Busan 609-735, Korea

³Department of Physics, Konan University, Kobe, Hyogo 658-8501, Japan

⁴Kansai Photon Science Institute, Japan Atomic Energy Agency, Kizu, Kyoto 619-0215, Japan

⁵Institute of Physics, Academia Sinica, Taipei 11529, Taiwan

⁶Japan Synchrotron Radiation Research Institute, Mikazuki, Hyogo 679-5198, Japan

⁷Department of Physics and Astrophysics, Nagoya University, Nagoya, Aichi 464-8602, Japan

⁸School of Physics, Seoul National University, Seoul, 151-747, Korea

⁹Department of Physics, Kyoto University, Kyoto 606-8502, Japan

¹⁰Department of Physics And Astronomy, Ohio University, Athens, Ohio 45701, USA

¹¹Laboratory of Nuclear Science, Tohoku University, Sendai, Miyagi 982-0826, Japan

¹²Department of Physics, Yamagata University, Yamagata 990-8560, Japan

¹³Department of Physics, Chiba University, Chiba 263-8522, Japan

¹⁴Wakayama Medical University, Wakayama, Wakayama 641-8509, Japan

¹⁵Department of Applied Physics, Miyazaki University, Miyazaki 889-2192, Japan

¹⁶Department of Applied Physics, National Defense Academy, Yokosuka 239-8686, Japan

¹⁷Department of Physics, Tokyo Institute of Technology, Tokyo 152-8551, Japan

¹⁸Department of Physics, Chung-Yuan Christian University, Chung-Li 32023, Taiwan

¹⁹Department of Physics, Osaka University, Toyonaka, Osaka 560-0043, Japan

²⁰Department of Physics, University of Saskatchewan, Saskatoon, Saskatchewan, Canada

²¹School of Physics and Astronomy, University of Minnesota, Minneapolis, Minnesota 55455, USA

²²Joint Institute of Nuclear Research, 141980, Dubna, Russia

²³Akita Research Institute of Brain and Blood Vessels, Akita 010-0874, Japan

²⁴Institute for Protein Research, Osaka University, Suita, Osaka 565-0871, Japan and

²⁵National Superconducting Cyclotron Laboratory, Michigan State University, MI 48824, USA

(Dated: October 26, 2018)

Differential cross sections and photon-beam asymmetries for the $\vec{\gamma}p \rightarrow K^+\Lambda(1520)$ reaction have been measured with linearly polarized photon beams at energies from the threshold to 2.4 GeV at $0.6 < \cos\theta_{\text{CM}}^K < 1$. A new bump structure was found at $W \simeq 2.11$ GeV in the cross sections. The bump is not well reproduced by theoretical calculations introducing a nucleon resonance with $J \leq \frac{3}{2}$. This result suggests that the bump might be produced by a nucleon resonance possibly with $J \geq \frac{5}{2}$ or by a new reaction process, for example an interference effect with the ϕ photoproduction having a similar bump structure in the cross sections.

PACS numbers: 13.60.Le, 13.88.+e, 14.20.Gk, 14.20.Jn, 14.40.Aq, 25.20.Lj

Strangeness photoproduction is an important tool to gain a deeper understanding of the nature of baryon resonances. Theoretically, constituent quark models predict more nucleon resonances than those observed in pion scattering reactions. Quark model studies suggest that these missing resonances couple to strangeness channels which are not only KY ($Y=\Lambda$ or Σ) but also KY^* ($Y^*=\Lambda^*$ or Σ^*) [1]. Some nucleon resonances have been observed at the near-threshold energies in the KY photoproduction [2–4]. The threshold for the KY^* photoproduction is relatively high compared with that for the

πN , ηN , and KY photoproduction. Therefore, photoproduction leading to the KY^* state is a good way to investigate poorly understood nucleon resonances with a heavy mass.

Another physics interest in the KY^* reaction is that the bump structure found at $E_\gamma \sim 2$ GeV in the cross sections for the ϕ photoproduction [5] might be explained by the coupled-channel or interference effects with relevant reactions [6]. The cause of the bump has not been clarified yet. Measuring cross sections and spin observables for these relevant reactions, which have similar energy

thresholds and final states, could play an important role in clarifying the cause of the bump. The $K^+\Lambda(1520)$ photoproduction is one of the best reactions to satisfy the requirements for such a study.

The reaction mechanism of the $K^+\Lambda(1520)$ photoproduction is often described in terms of hadron exchanges, with N and N^* in the s -channel, Y and Y^* in the u -channel, and K and K^* in the t -channel. Recent theoretical studies suggest that the contact term (to satisfy the gauge invariance) is dominant and the s -channel contribution is negligibly small in the $K^+\Lambda(1520)$ reaction [7, 8]. Another theoretical study suggests that the K^* exchange contribution is small [9]. On the other hand, previous $K^+\Lambda(1520)$ photoproduction data at the center-of-mass (CM) energies ($W=\sqrt{s}$) of $W=2.48$ - 3.14 GeV ($E_\gamma=2.8$ - 4.8 GeV) show that K^* exchange in the t -channel is dominant [10]. Recent $K^+\Lambda(1520)$ electroproduction data at $W=1.95$ - 2.65 GeV show that contributions from K and K^* exchanges are roughly equal [11]. Therefore, additional data with new observables are needed for solving this controversial situation. The photon-beam asymmetry (Σ) for $K^+\Lambda(1520)$ photoproduction has some unique features. Nam *et al.* predict that $\Sigma = -1$ or $\Sigma > 0$ if the K or K^* meson is exchanged in the t -channel, respectively [8]. The contact term, u -channel, and s -channel N exchange contributions give almost zero asymmetries. Hence, a measurement of the Σ asymmetry provides strong constraints in understanding the $K^+\Lambda(1520)$ photoproduction mechanism.

In the past, experimental data for hyperon photoproduction at the near-threshold energies were available only for the $K^+\Lambda$ and $K^+\Sigma^0$ states [2-4, 12, 13]. Recently, new experimental results for $K^0\Sigma^+$ [14], $K^+\Sigma^-$ [15], $K^*\Sigma^+$ [16, 17], $K^+\Lambda(1405)$ [18], and $K^+\Sigma^-(1385)$ [19] have been reported. However, there are only two old published results on $K^+\Lambda(1520)$ photoproduction at energies of $E_\gamma=2.8$ - 4.8 GeV [10] and $E_\gamma=11$ GeV [20]. New experimental data near the $K^+\Lambda(1520)$ threshold are useful to investigate the possibility of new nucleon resonances, to obtain key information for clarifying the cause of the bump found in the ϕ photoproduction, and to understand the $K^+\Lambda(1520)$ reaction mechanism. In this Letter, we present, for the first time, differential cross sections and photon-beam asymmetries for the $\vec{\gamma}p \rightarrow K^+\Lambda(1520)$ reaction at $0.6 < \cos\theta_{\text{CM}}^K < 1$ at the near-threshold energies.

The experiment was carried out using the laser-electron photon facility at SPring-8 (LEPS) [21]. The energy range of tagged photons was 1.5-2.4 GeV, and the polarization of linearly polarized photons was 52-90% at 1.5-2.4 GeV. We used a liquid hydrogen (LH₂) target with an effective length of 16 cm. Charged particles produced at the target were detected at forward angles with the LEPS spectrometer system for trajectory tracking. Time-of-flight information was obtained for each charged particle track. The start signal was produced by a plastic scintillator (SC) located behind the target, and the stop signal was produced by an array of 40 plastic scintillators at the downstream of the spectrometer. The K^+ meson

was identified from its mass, within 3σ where σ is the momentum dependent mass resolution. The data sample with the single K^+ meson was analyzed.

Figure 1 shows the missing mass ($MM_{\gamma K^+}$) spectrum for the $p(\vec{\gamma}, K^+)X$ reaction. The wide lower-mass peak corresponds to the $\Sigma^0(1385)$ and $\Lambda(1405)$ production, and the narrow higher-mass peak corresponds to the $\Lambda(1520)$. The $\Lambda(1520)$ yield was obtained by fitting the peaks in the missing mass spectrum. The photon energy region from the threshold to 2.4 GeV was divided into 15 bins and the K^+ polar angle region in the CM system was divided into 4 bins. The peak shape of each hyperon resonance was estimated by GEANT simulations. Breit-Wigner shapes with masses of 1.384, 1.407, and 1.520 GeV and widths of 36, 50, and 16 MeV were used to generate the $\Sigma^0(1385)$, $\Lambda(1405)$, and $\Lambda(1520)$ hyperon resonances, respectively [22]. The masses and widths of the hyperon resonances are uncertain [22], and these uncertainties were evaluated as systematic errors. The peak shape was reproduced by the missing mass of the $p(\gamma, K^+)X$ reaction in the simulations including the experimental resolution. The peak shape was fixed in the fit to the experimental missing mass spectrum and the height of the peak was adjusted as a free parameter. There is a small bump at 1.66 GeV, probably due to the $\Sigma^0(1660)$. Since the mass and width of the $\Sigma^0(1660)$ are not well known, the same peak shape as the $\Lambda(1520)$ was used, but with its position fixed at 1.660 GeV in the fit.

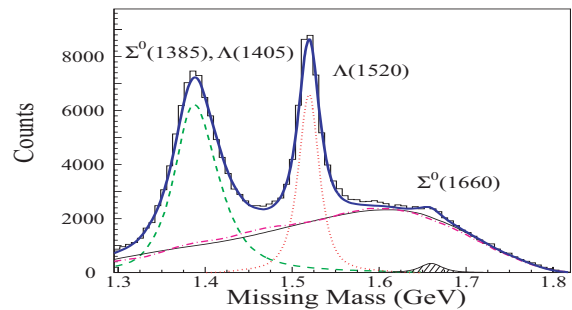


FIG. 1: Missing mass of the $p(\gamma, K^+)X$ reaction at $E_\gamma=1.5$ - 2.4 GeV and $0.6 < \cos\theta_{\text{CM}}^K < 1$. The thick solid curve is the result of the fit using the polynomial background (thin solid curve). The dashed, dotted, and hatched curves correspond to $\Sigma^0(1385)/\Lambda(1405)$, $\Lambda(1520)$, and $\Sigma^0(1660)$ productions, respectively. The dotted-dashed curve is the background obtained by the fit using simulation curves.

The background under the hyperon peaks was fit by using a polynomial function. The $\gamma p \rightarrow K^+\pi Y$, K^*Y , K^+KN , and ϕp reactions account for the majority of the background under the hyperon peaks in the simulation studies. The $K^+\pi Y$ and K^*Y reactions are considered to be dominant at $MM_{\gamma K^+} < 1.5$ GeV, while the ϕp reaction is dominant at $MM_{\gamma K^+} > 1.5$ GeV. As a result of the fit, the $\Lambda(1520)$ yield was obtained for each incident photon energy and angular bin. The differential cross sections for the $K^+\Lambda(1520)$ reaction were obtained by using the

same method in Ref. [4].

A fit with background curves generated for the $\gamma p \rightarrow K^+\pi Y$, K^*Y , K^+KN , and ϕp reactions by the simulations makes a difference of at most $0.1 \mu\text{b}$ for the $K^+\Lambda(1520)$ cross sections. The sum of the background curves is shown in Fig. 1. Systematic uncertainties of the shape, mass, and width of the $\Lambda(1520)$, $\Lambda(1405)$, and $\Sigma^0(1385)$ resonances cause uncertainties of $0.04 \mu\text{b}$ at $W < 2.15 \text{ GeV}$ and $0.07 \mu\text{b}$ at $W > 2.15 \text{ GeV}$. Uncertainties of the target thickness, photon flux, and detector acceptance are 1%, 5%, and 3%, respectively. The π^+ contamination in the particle identification of the K^+ is negligibly small. When the K^+ is detected at forward angles, the vertex resolution becomes poor. The contamination of events from the SC in the vertex selection of the LH₂ target is smaller than 3% at $W > 2.04 \text{ GeV}$ and smaller than 7% at $W < 2.04 \text{ GeV}$.

The differential cross sections for the $\bar{\gamma}p \rightarrow K^+\Lambda(1520)$ reaction are shown in Fig. 2. The cross sections increase with the CM energy near the threshold. It is quite interesting that the experimental cross sections rapidly decrease at around $W=2.2 \text{ GeV}$ and a clear bump structure is observed at the K^+ angles of $0.8 < \cos\theta_{\text{CM}}^K$. The rapid decrease at around $W=2.2 \text{ GeV}$ is much larger than the statistical and systematic errors. This bump energy is similar to the energy where another bump was found in the ϕ photoproduction [5]. Note that the bump at this energy is not observed in the $K^+\Lambda(1116)$ [4], $K^+\Sigma^0$ [4, 15], $K^+\Sigma^-$ [15], or $K^+\Sigma^-(1385)$ [19] cross sections obtained using the same method.

The $K^+\Lambda(1520)$ cross sections are compared with the prescaled $K^+\Lambda(1116)$ cross sections [3] as a function of the excess energy in Fig. 3. The clear bump structure found in the present $K^+\Lambda(1520)$ cross sections is not seen in the forward-angle $K^+\Lambda(1116)$ cross sections, which suggests that the reaction mechanism is different between the two reactions at these near-threshold energies.

Two theoretical calculations, which are based on an effective Lagrangian approach, by Titov *et al.* [23] and Nam *et al.* [7] monotonically increase with the CM energy up to $W \sim 2.3 \text{ GeV}$ in Fig. 2(a, b, c, d). The calculations by Titov *et al.* are not tuned to fit the data. The calculations by Nam *et al.* are dominated by the contact term contribution. Although the results of the calculations by Nam *et al.* approach the present data by optimizing the cutoff parameter, the rapid decrease associated with the bump cannot be reproduced. The agreement with the present data is poor.

As one possibility, we perform new calculations to describe the present data by introducing a nucleon resonance with a free mass and a width [24], although the angular coverage of the data is inadequate to obtain strong evidence for the nucleon resonance. The spins and parities of $J^\pi = \frac{1}{2}^\pm$ and $\frac{3}{2}^\pm$ for the nucleon resonance are considered. Contributions from the nucleon resonance with a spin higher than $\frac{3}{2}$ are not included due to theoretical ambiguities. The angular distributions of the $J^\pi = \frac{1}{2}^\pm$ and $\frac{3}{2}^\pm$ states are almost flat. The $J^\pi = \frac{3}{2}^+$

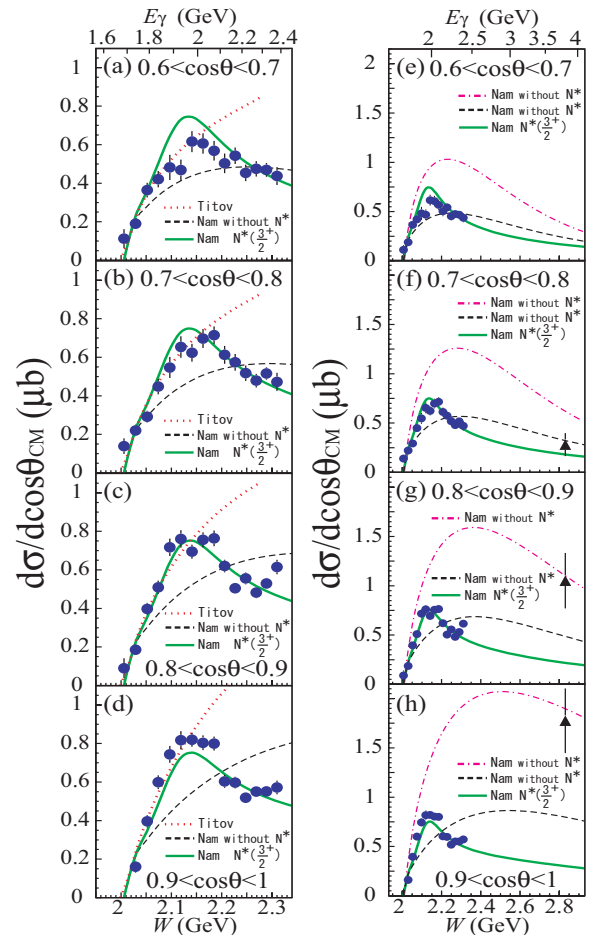


FIG. 2: Differential cross sections for the $K^+\Lambda(1520)$ reaction at (a, e) $0.6 < \cos\theta_{\text{CM}}^K < 0.7$, (b, f) $0.7 < \cos\theta_{\text{CM}}^K < 0.8$, (c, g) $0.8 < \cos\theta_{\text{CM}}^K < 0.9$, and (d, h) $0.9 < \cos\theta_{\text{CM}}^K < 1$. The circles are the present data. The circles in the left and right figures are the same data. The triangles are the Daresbury data ($E_\gamma=2.8\text{-}4.8 \text{ GeV}$) [10]. The solid and dashed curves are the results of calculations fitting to the present data by Nam *et al.* with and without a nucleon resonance ($J^\pi = \frac{3}{2}^+$), respectively [24]. The dotted-dashed curves are the results of calculations fitting to the Daresbury data by Nam *et al.* [7]. The dotted curves are the results of calculations by Titov *et al.* [23].

state gives a better reduced $\chi^2(1.37)$ for the fit than the other states, and the energy dependence of the bump is reproduced by the solid curves of Fig. 2. However, the angular distribution of the bump is not well reproduced. The theoretical calculations estimate the cross sections at backward K^+ angles to be about $0.7 \mu\text{b}$ that overestimates the experimental cross sections [25] by 2-3 times. The bump is not observed in the cross sections of the backward K^+ angles [25].

As a result of the fit, the mass and width of the $J^\pi = \frac{3}{2}^+$ nucleon resonance are obtained as 2.11 GeV and 140 MeV , respectively. Nucleon resonances with similar

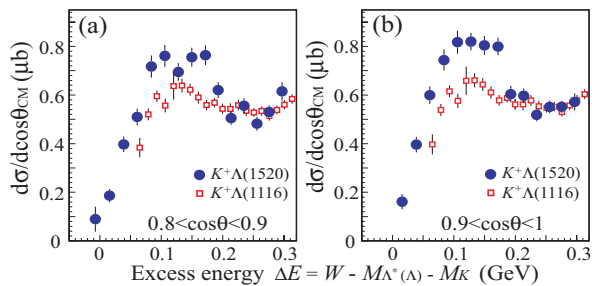


FIG. 3: Differential cross sections for the $K^+\Lambda(1520)$ (circles) reaction at (a) $0.8 < \cos \theta_{\text{CM}}^K < 0.9$ and (b) $0.9 < \cos \theta_{\text{CM}}^K < 1$ as a function of the excess energy (ΔE). The squares are prescaled differential cross sections for the $K^+\Lambda(1116)$ reaction at $0.8 < \cos \theta_{\text{CM}}^K < 0.9$ [3]. The prescale factors of 0.263 for (a) and 0.271 for (b) are used to fit the $K^+\Lambda(1116)$ cross sections to the $K^+\Lambda(1520)$ cross sections at $0.2 \text{ GeV} < \Delta E < 0.3 \text{ GeV}$. There are no $K^+\Lambda(1116)$ data at $0.9 < \cos \theta_{\text{CM}}^K < 1$.

masses are $D_{13}(2080)$ with 2-star status, $S_{11}(2090)$ and $P_{11}(2100)$ with 1-star status, and $G_{17}(2190)$ with 4-star status in the PDG particle listings [22]. In the listings, there is no corresponding nucleon resonance at 2.11 GeV. Note that most of the widths measured for the nucleon resonances in the listings are much wider than 140 MeV. Quark model studies predict that a new $J^\pi = \frac{5}{2}^-$ state with a similar mass of 2.08 GeV may be visible in the $K^+\Lambda(1520)$ reaction [1]. Theoretical improvements for introducing a nucleon resonance with spins higher than $\frac{3}{2}$ are important to judge whether the bump is produced by the nucleon resonance or not.

Another possible explanation for the bump is a new reaction process, for example, an interference effect between the ϕ and $\Lambda(1520)$ photoproduction reactions might produce the bump because both reactions have this feature in the cross sections at similar energies [5]. Coupled-channel effects are unlikely to reproduce the strength and the angular distribution of the bump [26].

Typical cross sections for hyperon photoproduction, such as $K^+\Lambda(1116)$ and $K^+\Sigma^0(1193)$, show a gradual decrease with increasing the CM energy [13]. A gradual decrease in the $K^+\Lambda(1520)$ cross sections [10] is reproduced by the calculations of Nam *et al.* [7, 24] as shown by all the curves of Fig. 2(e, f, g, h). Although the connection between the present data and the Daresbury data seems to be smooth at $0.7 < \cos \theta_{\text{CM}}^K < 0.8$, the Daresbury data at $0.8 < \cos \theta_{\text{CM}}^K$ are not smoothly extrapolated from the present data as shown by the solid curves of Fig. 2(f, g, h). The differences between the Daresbury data and the solid curves are larger than three standard deviations at $0.8 < \cos \theta_{\text{CM}}^K$. Calculations that would agree well with both data sets are very difficult at present. New experimental data ($W=2.3\text{-}2.8 \text{ GeV}$) are desired to fill the gap between these two data sets.

By using vertically and horizontally polarized photon beams, the photon-beam asymmetry has been shown to be insensitive to the spectrometer acceptance [4, 12].

The asymmetry (Σ) is given as $P_\gamma \Sigma \cos 2\phi = (N_v - N_h)/(N_v + N_h)$, where N_v and N_h are the $\Lambda(1520)$ yields with the vertically and horizontally polarized photons, respectively. P_γ is the polarization degree of the photon beam, and ϕ is the K^+ azimuthal angle defined by the angle between the reaction plane and the horizontal plane. The photon energy region from the threshold to 2.4 GeV was divided into 7 bins and the K^+ azimuthal angle region was divided into 9 bins. The K^+ polar angle region was not divided. The $\Lambda(1520)$ yields were obtained for each energy and angular bin by fits to the missing mass.

Figure 4(a) shows the K^+ azimuthal angle distribution of the ratio $(N_v - N_h)/(N_v + N_h)$ at $W=2.28\text{-}2.32 \text{ GeV}$. The amplitude of the fit curve was divided by P_γ and the asymmetry Σ was obtained. Systematic uncertainties of the shape, mass, and width of the $\Lambda(1520)$, $\Sigma^0(1385)$, $\Lambda(1405)$, and $\Sigma^0(1660)$ hyperon resonances cause the uncertainty, $\delta\Sigma=0.05$. A fit with background curves generated for the $\gamma p \rightarrow K^+\pi Y$, K^*Y , K^+KN , and ϕp reactions by the simulations is consistent within the statistical error. The effect of the π^+ contamination in the K^+ selection is negligible. When the K^+ is detected at forward angles, the vertex resolution becomes poor. The effect of the contamination of events from the SC in the vertex selection of the LH₂ target is also negligible. The attenuation of the asymmetry by the finite number of the azimuthal angle bins (9 bins) is about $\delta\Sigma=0.015$. The systematic uncertainty of the measurement of the laser polarization is $\delta\Sigma=0.02$.

Figure 4(b) shows the photon-beam asymmetries for the $K^+\Lambda(1520)$ reaction at $0.6 < \cos \theta_{\text{CM}}^K < 1$ in comparison with those for the $K^+\Lambda(1116)$ reaction at $\cos \theta_{\text{CM}}^K \sim 0.85$ [27]. The $K^+\Lambda(1520)$ asymmetries are near zero at $W < 2.2 \text{ GeV}$ and increase gradually with the CM energy. The small positive values at $W > 2.2 \text{ GeV}$ might indicate that the contribution from the K^* exchange is larger than that from the K exchange. The asymmetries for the $K^+\Lambda(1520)$ reaction are smaller than those for the $K^+\Lambda(1116)$ reaction. One reason of the small $K^+\Lambda(1520)$ asymmetries is that the K^* exchange contribution may be smaller than that in the $K^+\Lambda(1116)$ reaction. The contact term and K exchange contributions make the $K^+\Lambda(1520)$ asymmetries smaller. This comparison suggests that the $K^+\Lambda(1520)$ reaction mechanism is different from the $K^+\Lambda(1116)$ reaction mechanism at these near-threshold energies.

The $K^+\Lambda(1520)$ asymmetry data are compared with the results of theoretical calculations by Nam *et al.* with and without a nucleon resonance ($J^\pi = \frac{1}{2}^\pm$ or $\frac{3}{2}^\pm$) for the bump [24]. The calculations use the parameters obtained from fits to the present cross sections. There is no significant difference between the results of these calculations as shown in Fig. 4(b). Since all theoretical asymmetries are close to zero and agree with the data at $W < 2.2 \text{ GeV}$, we cannot judge whether the bump is due to a nucleon resonance or not. The measurement of additional spin observables is needed to clarify the cause of the bump. The calculations underestimate the data by 1-3 standard

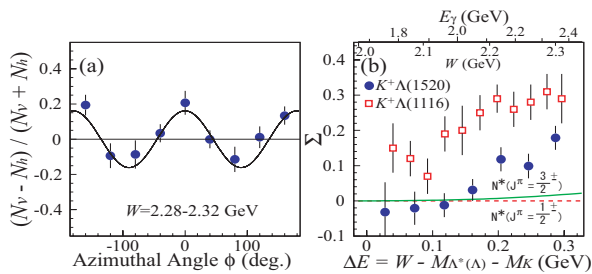


FIG. 4: (a) Azimuthal angle distribution of the ratio $(N_v - N_h)/(N_v + N_h)$ for the $K^+\Lambda(1520)$ reaction at $W=2.28-2.32$ GeV. (b) Photon-beam asymmetries for the $K^+\Lambda(1520)$ (circles) and $K^+\Lambda(1116)$ (squares) [27] reactions as a function of the excess energy (ΔE). The dashed and solid curves are the results of calculations for the $K^+\Lambda(1520)$ by Nam *et al.* introducing the $J^\pi = \frac{1}{2}^\pm$ and $J^\pi = \frac{3}{2}^\pm$ nucleon resonances, respectively [24]. The parity for the resonances does not change the theoretical asymmetries significantly. The result of calculations without a nucleon resonance is almost identical to the solid curve.

deviations including the systematic uncertainties above the bump energy. The contribution from the K^* exchange is estimated to be larger than that obtained from fits to just the cross section data.

In summary, we have measured differential cross sections and photon-beam asymmetries for the $\bar{\gamma}p \rightarrow K^+\Lambda(1520)$ reaction. A bump structure was found in the cross sections. As one possible explanation, we introduce a nucleon resonance with $J \leq \frac{3}{2}$ in the theoretical calculations dominated by the contact term contribution, although the angular coverage of our data is inadequate to obtain strong evidence for the nucleon resonance. The calculations reproduce the energy depen-

dence of the bump at forward K^+ angles, but fail to reproduce the angular distribution of the bump. Further theoretical calculations with $J \geq \frac{5}{2}$ resonances are necessary to examine the presence of a nucleon resonance. Another possible explanation is that the bump might be produced by a new reaction process, for example an interference effect with ϕ photoproduction. The $K^+\Lambda(1520)$ asymmetries have small positive values at $W > 2.2$ GeV, which may indicate that the contribution from the K^* exchange is larger than that from the K exchange. The asymmetries for the $K^+\Lambda(1520)$ reaction are smaller than those for the $K^+\Lambda(1116)$ reaction, which confirms that the $K^+\Lambda(1520)$ reaction mechanism is different from the $K^+\Lambda(1116)$ reaction mechanism at these near-threshold energies. The present result stimulates future experimental and theoretical studies for not only the KY^* photoproduction reaction but also other relevant reactions with wider angular coverage, and will advance our understanding of the hadron photoproduction and baryon resonance.

The authors thank the SPring-8 staff for supporting the experiment. We thank Mr. S. Ozaki for fruitful discussions. This research was supported in part by the Ministry of Education, Science, Sports and Culture of Japan, by the National Science Council of Republic of China (Taiwan), by the National Research Foundation of Korea, and by National Science Foundation (USA).

^aPresent address: Faculty and Graduate School of Engineering, Hokkaido University, Sapporo 060-8628, Japan.

^bPresent address: Nuclear Physics Institute, Moscow State University, Moscow, 119899, Russia.

^cPresent address: Illinois Institute of Technology, Chicago, IL 60616, USA.

-
- [1] S. Capstick and W. Roberts, Phys. Rev. D **58**, 074011 (1998).
[2] T. Mart and C. Bennhold, Phys. Rev. C **61**, 012201(R) (1999).
[3] J.W.C. McNabb *et al.*, Phys. Rev. C **69**, 042201 (2004).
[4] M. Sumihama *et al.*, Phys. Rev. C **73**, 035214 (2006).
[5] T. Mibe *et al.*, Phys. Rev. Lett. **95**, 182001 (2005).
[6] S. Ozaki, A. Hosaka, H. Nagahiro, and O. Scholten, Phys. Rev. C **80**, 035201 (2009).; Private communication.
[7] S.i. Nam, A. Hosaka, and H.-Ch. Kim, Phys. Rev. D **71**, 114012 (2005).
[8] S.i. Nam, K.S. Choi, A. Hosaka, and H.-Ch. Kim, Phys. Rev. D **75**, 014027 (2007).
[9] H. Toki, C. Garcia-Recio, and J. Nieves, Phys. Rev. D **77**, 034001 (2008).
[10] D.P. Barber *et al.*, Z. Phys., **7**, 17 (1980).
[11] S.P. Barrow *et al.*, Phys. Rev. C **64**, 044601 (2001).
[12] R.G.T. Zegers *et al.*, Phys. Rev. Lett. **91**, 092001 (2003).
[13] R. Bradford *et al.*, Phys. Rev. C **73**, 035202 (2006).
[14] R. Castelijns *et al.*, Eur. Phys. J. A **35**, 39 (2008).
[15] H. Kohri *et al.*, Phys. Rev. Lett. **97**, 082003 (2006).
[16] I. Hleiqawi *et al.*, Phys. Rev. C **75**, 042201(R) (2007).
[17] M. Nanova *et al.*, Eur. Phys. J. A **35**, 333 (2008).
[18] M. Niiyama *et al.*, Phys. Rev. C **78**, 035202 (2008).
[19] K. Hicks *et al.*, Phys. Rev. Lett. **102**, 012501 (2009).
[20] A.M. Boyarski *et al.*, Phys. Lett. B **34**, 547 (1971).
[21] T. Nakano *et al.*, Nucl. Phys. A **684**, 71 (2001).
[22] W.-M. Yao *et al.*, J. Phys. G **33**, 1 (2006).
[23] A.I. Titov, B. Kämpfer, S. Daté, and Y. Ohashi, Phys. Rev. C **72**, 035206 (2005).
[24] S.i. Nam and A. Hosaka, Private communication.
[25] N. Muramatsu *et al.*, Phys. Rev. Lett. **103**, 012001 (2009).
[26] S. Ozaki, Private communication.
[27] A. Lleres *et al.*, Eur. Phys. J. A **31**, 79 (2007).